

---

**PAT PACKAGE DROP TEST—  
TARGET ACCURACY ANALYSIS**

December 31, 1989

---

R. E. Glaser, J. H. VanSant

Prepared for  
U.S. Nuclear Regulatory Commission

9010050115 900927  
PDR ORG NEMA  
PDC

## DISCLAIMER

This document was prepared as an account of work sponsored by an agency of the United States Government. Neither the United States Government nor any agency thereof, nor any of their employees, makes any warranty, expressed or implied, or assumes any legal liability or responsibility for the accuracy, completeness, or usefulness of any information, apparatus, product, or process disclosed, or represents that its use would not infringe privately owned rights. Reference herein to any specific commercial product, process, or service by trade name, trademark, manufacturer, or otherwise, does not necessarily constitute or imply its endorsement, recommendation, or favoring by the United States Government or any agency thereof. The views and opinions of authors expressed herein do not necessarily state or reflect those of the United States Government or any agency thereof.

This work was supported by the United States Nuclear Regulatory Commission under a Memorandum of Understanding with the United States Department of Energy.

PATC-IR 89-10

---

PAT PACKAGE DROP TEST—  
TARGET ACCURACY ANALYSIS

December 31, 1989

---

R. E. Glaser, J. H. VanSant

Prepared for  
U.S. Nuclear Regulatory Commission







## ABSTRACT

In this report we present the results of a statistical analysis of the target accuracy of a plutonium air transport (PAT) package drop test conducted in accordance with criteria specified in Ref. 1. The test package must be released from an aircraft at a predetermined location and fall within a designated target area to ensure safety of people on the ground and successful photography of the package during its descent and impact. The probable target miss distance is estimated by using an example package drop methodology and its associated parameter values and assumed errors. The example drop method provides for dropping a 2.6-Mg test package from a C-130 aircraft flying into the wind at an altitude of 7.6 km (25,000 ft). For the drop from the aircraft, the package is fastened to a pallet that is connected to a drag parachute. At a preset time after the drop, the package is automatically released from the pallet for free fall. We obtained probability distributions of the target miss distance by Monte Carlo simulation. The results indicate that the probability that a test package will impact within an 881-m radius from the target is 99%. The mean target miss distance is estimated to be 413 m.



## TABLE OF CONTENTS

	<u>Page</u>
ABSTRACT.....	iii
1. INTRODUCTION .....	1
2. PACKAGE DROP METHOD.....	2
2.1 Drop Test Aircraft.....	2
2.2 Predrop Calculations.....	2
2.3 Pallet/Package Assembly.....	2
2.4 Approach to the Drop Point.....	4
2.5 Package Release.....	4
2.6 Package Free Fall.....	4
2.7 Parameter Values.....	7
2.8 Deviations.....	8
3. PROBABILITY DISTRIBUTION OF TARGET MISS DISTANCE.....	9
3.1 Method.....	9
3.2 Results.....	20
4. CONCLUSIONS.....	35
5. REFERENCES.....	35



## 1. INTRODUCTION

Section 5062 of Public Law 100-203 defines specific tests required for plutonium air transport (PAT) packages designed for transporting plutonium from one foreign country to another through U.S. airspace. Criteria for these tests are proposed in Ref. 1. The subject of this report is one of these tests — an air drop of a PAT test package from a test aircraft. In this test, the package must fall into a designated target area where the soil properties have been surveyed, a safety buffer zone has been defined, and tracking cameras can follow the package to impact. The target miss distance of the PAT package drop must be as small as can be practically achieved so that quality photographs of the impact can be obtained. These photographs will be used to determine the impact velocity and to study dynamic events that occur at impact.

In this report we present the method and results of a probabilistic study of the target accuracy of an example drop test. Assumptions used in the study include an example package, an example drop method, and associated test parameter values and errors. The results indicate a conservative estimate of accuracy for the example case. Should a drop test program be implemented, the same analysis methodology could be used to determine an expected probable miss distance distribution for the actual package, drop method, and associated parameter values.

This study was preceded by a ballistic analysis of the drop test (Ref. 2). Free-fall trajectories were computed for example PAT packages dropped from aircraft. Also, trajectory calculations were performed for test packages with drag parachutes attached. Effects accounted for include:

- Package geometry and mass.
- Package aerodynamic characteristics.
- Drop aircraft velocity, heading, and altitude.
- Air density variation with altitude.
- Wind velocity variation with altitude.
- Parachute drag characteristics.

We used data derived by the ballistic analysis in the present study of target accuracy. Principal values are: required impact velocity, corresponding drop altitude, and horizontal displacement sensitivities.

## **2. PACKAGE DROP METHOD**

We base our example method for dropping PAT test packages and achieving the required impact conditions in part on information obtained from personal contacts at U.S. Air Force test ranges. The example drop load of 2.8 Mg (6160 lb) must be dropped from 7.6 km (25,000 ft); either a C-130 or B-52 aircraft could meet this requirement. Because the target accuracy improves with decreasing horizontal velocity of the test package, we use drag parachutes to reduce the horizontal velocity. The following sections provide details of our example drop method.

### **2.1 Drop Test Aircraft**

A C-130 aircraft is the example vehicle chosen for transporting the PAT test package to a prescribed altitude. This aircraft has a rear cargo door that can be remotely opened and closed in flight. The C-130 is designed to air-drop military paratroops, supplies, and equipment. It can be flown with partially extended landing flaps to achieve a reduced airspeed: e.g., 100 m/s (194 knots) true air speed at 7.6 km altitude. Under these conditions, the aircraft would be flying nose-up, which would facilitate the release of the test package assembly out the rear cargo door. The package assembly would also be supported by an inclined roller platform and would be ejected with an air cylinder to increase its exit velocity. To improve target accuracy, it is desirable to minimize both package exit time and its relative ground velocity [with drag parachutes].

### **2.2 Predrop Calculations**

Prior to the drop, wind and atmospheric data from the drop area must be obtained with appropriate instruments, such as sounding balloons or weather radar. In particular, altitude profiles of wind velocity and direction and air density are needed. A computer code uses these data to predict test package trajectory and impact velocity (Ref. 2). Computations are performed to determine the required release altitude and direction. (Drop test criteria in Ref. 1 specify that the test package's impact velocity shall not be less than its impact velocity at sea level would be if it were released at the maximum cruising altitude of the designated cargo aircraft.) The trajectory analysis must include drag coefficient data obtained from previous aerodynamic tests on a prototype model of the test package. Also required are drag coefficient values for the parachutes used in the package drop. Values of these drag coefficients have been published (Refs. 3 and 4).

### **2.3 Pallet/Package Assembly**

The test package is fastened to a special pallet with tie-down straps that have explosive cutters attached. Also attached to the pallet are drag parachutes that reduce the velocity of the pallet/package assembly after it is released from the rear of the aircraft. The drag parachutes are deployed by a static line attached to the aircraft in such a way that when the pallet exits out the rear of the aircraft, the parachute



packs open. The static line is also connected to a timing device for ignition of the explosive cutters. This device is preset for a time period beginning at release of the pallet/package assembly from the aircraft. Figure 1 shows the conceptual design of the pallet/package assembly.

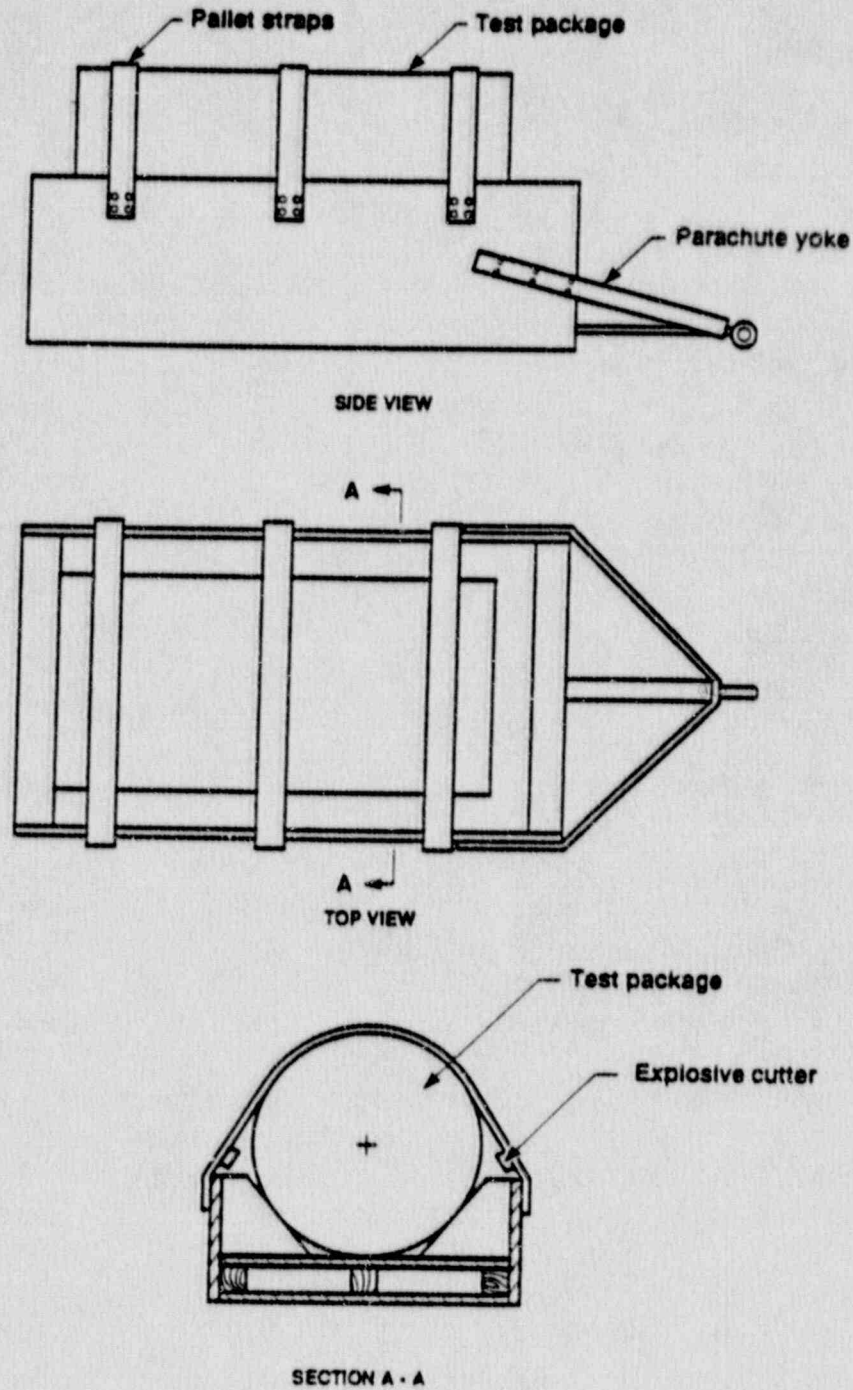


Fig. 1. A conceptual pallet for dropping a PAT test package.



## 2.4 Approach to the Drop Point

On the way to the drop point for the test package, the aircraft is flown at predetermined altitude, speed, and direction. The direction should be into the wind so that the ground speed will be reduced. We assume an example wind profile of 45 m/s (100 mph) at an altitude of 10.7 km (35,000 ft) that decreases exponentially to 7.5 m/s (17 mph) at ground level (Ref. 5) and that a ground radar tracking system in communication with the aircraft is used to direct the aircraft to a predetermined drop point. Before reaching the drop point, the aircraft is flown at the lowest flyable airspeed for the drop aircraft (about 67 m/s indicated airspeed). This will result in a nose-up attitude that causes the cargo deck to incline about 3° to the horizontal. The flight engineer opens the rear cargo door and releases the cargo tie-down latches by remote controls. At this stage, holding straps (or other suitable restraining devices) are still across the cargo bay to prevent the package from rolling out.

## 2.5 Package Release

When the aircraft reaches the prescribed location in airspace, the flight engineer engages a switch to release the cargo holding straps and to actuate the air cylinder. The pallet/package/parachute (PPP) assembly falls out of the aircraft, the drag parachutes are deployed, and the timing device is activated. The drag parachutes slow the pallet/package to a low velocity. When the set time has elapsed, the explosive cutters ignite and the package falls free of the pallet.

## 2.6 Package Free Fall

The assumed package geometry is a solid cylinder whose center of gravity is at its geometrical center. This configuration will allow the test package to fall in a tumbling mode. (In fact, tumbling cannot be prevented unless the centers of gravity and aerodynamic pressure are separated by a sufficient distance.) The ensuing trajectory of the package will depend on its aerodynamic characteristics and its initial direction, velocity, and altitude. Wind velocity and direction and air density, all of which are altitude-dependent, will also affect the package's trajectory. The final impact velocity will depend on these effects and the impact elevation. Figure 2 shows typical curves of velocity versus altitude for our example package released at selected altitudes (Ref. 2). Note that the impact velocity is nearly constant when the release altitude is greater than 6 km. Also, the package orientation (axial or side) has little effect on its velocity. There does not appear to be data on tumbling cylindrical shapes.

Figure 3 shows two trajectory curves for the example package when it is dropped according to the method described in Sections 2.4 and 2.5. One curve represents the aircraft flying into the standard wind when the package is dropped, and the other

curve represents the aircraft flying in zero wind conditions. Note that the horizontal distance traveled by the package in its fall is much less for zero wind than for the standard wind condition.

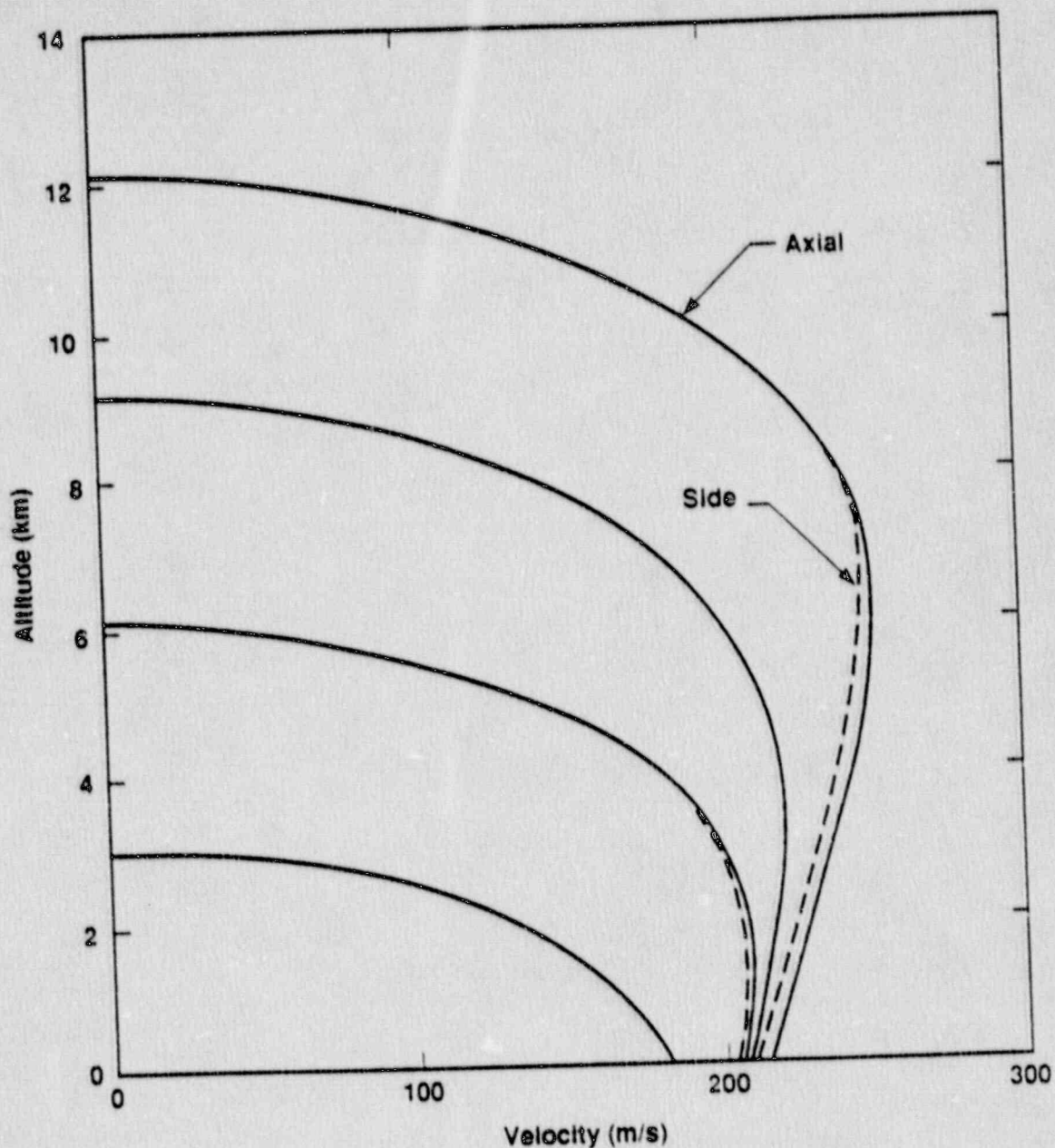


Fig. 2. Calculated velocity of the example PAT test package during free-fall when released at selected altitudes. Side and axial orientations are relative to the fall direction (Ref. 2).

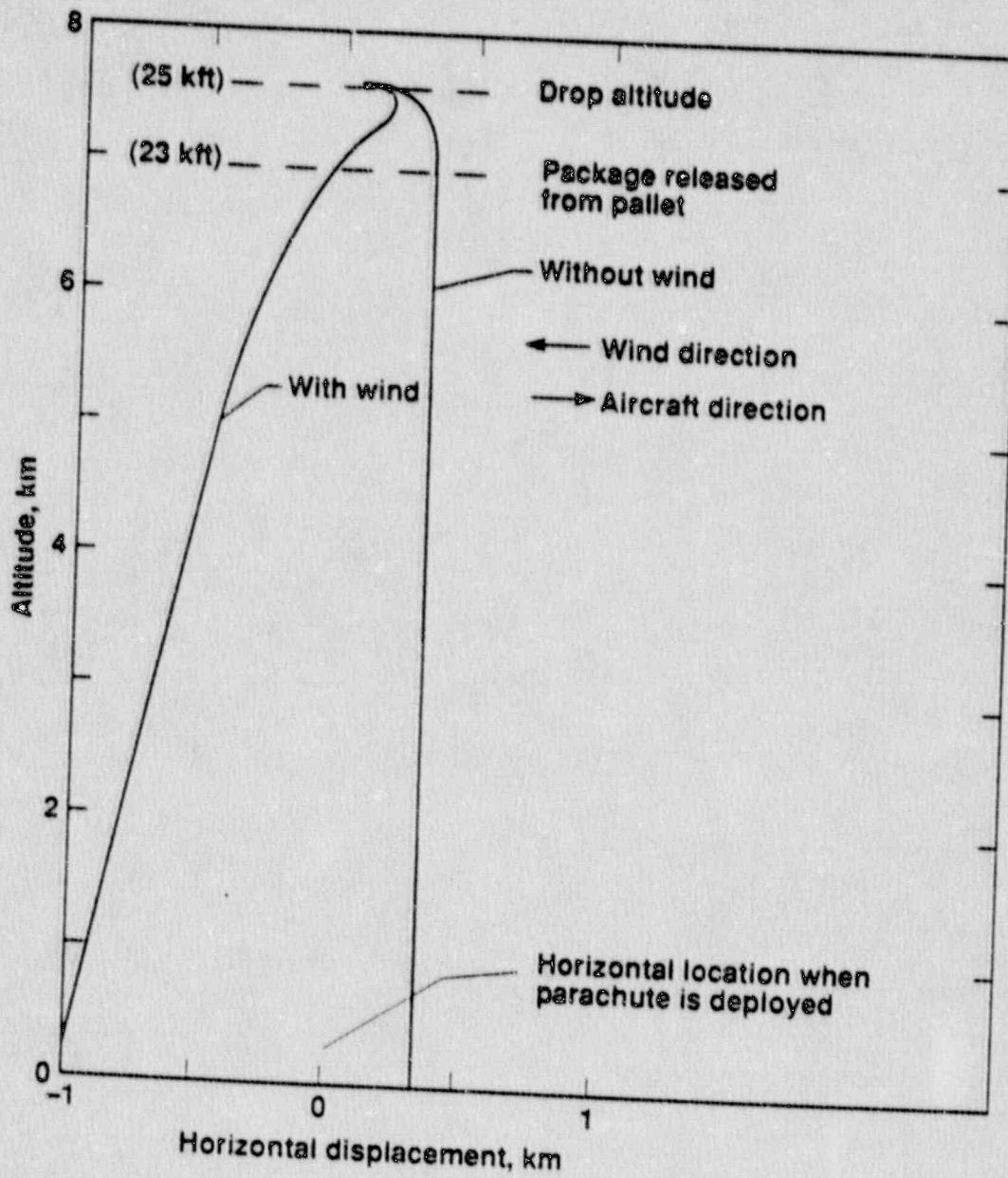


Fig. 3. Calculated trajectories of the example PAT test package during free-fall assuming standard wind velocity and no wind (Ref. 2).



## 2.7 Parameter Values

Table 1 gives the drop-test parameter values and conditions used in this study.

Table 1. Drop-test parameter values and conditions.

Item	Parameter/condition	Value
1.	Aircraft true airspeed	99.8 m/s (195 kt)
2.	Aircraft heading is into the wind	
3.	Aircraft ground speed	77.3 m/s (150 kt)
4.	Aircraft altitude	7.62 km (25,000 ft)
5.	Wind velocity at altitude of 7.62 km (25,000 ft)	22.2 m/s (43.7 kt)
6.	Wind velocity at altitude of 10.67 km (35,000 ft)	45.7 m/s (89 kt)
7.	PPP assembly exit velocity relative to the aircraft	1 m/s
8.	Reaction time of engineer to release PPP	0.5 s
9.	Time from PPP assembly release to parachute deployment	3 s
10.	Time from parachute deployment to package release	18 s
11.	Package velocity at drop from pallet	46.7 m/s
12.	Package direction of travel on drop from pallet (from horizontal with respect to aircraft heading)	117°
13.	Package altitude on drop from pallet	7.01 km (23,000 ft)
14.	Horizontal distance from PPP assembly release to parachute deployment	232 m
15.	Horizontal distance from parachute deployment to package drop	-85 m
16.	Horizontal distance from package drop to impact	-894 m
17.	Total horizontal distance from PPP assembly release to impact	-979 m
18.	Pallet weight	200 kg (440 lb)
19.	Package weight	2,600 kg
20.	Package diameter	1.2 m
21.	Package length	2.4 m
22.	Drag parachute diameter (deployed)	5 m
23.	Number of drag parachutes	2
24.	Maximum deceleration on package during drop	2.4 g
25.	Ground impact elevation	1,220 m (4,000 ft)
26.	Package impact velocity	208 m/s

Notes: A negative distance means a direction opposite to the aircraft flight direction. Items 7-10 and 18-22 have assumed values; other values are based on results of analyses or demonstrated performance.

## 2.8 Deviations

Table 2 lists assumed values of the 2- $\sigma$  half-band errors of control parameters used in this study. These values are not based on measurements — they are chosen by an engineering judgment of what should be expected. The assumed values represent a 95% probability that the achieved test parameter values will be within the assumed error bands of the specified parameter values.

Table 2. Half-band error values.

Item	Parameter/condition	Value
1.	Aircraft heading	1/2°
2.	Aircraft altitude	30 m (100 ft)
3.	Aircraft true airspeed	5 m/s (10 kt)
4.	Aircraft location (2-D space) (at time engineer receives signal to release PPP assembly)	60 m (200 ft)
5.	Reaction time of engineer to press release button	0.25 s
6.	Time for PPP assembly to exit the aircraft and parachutes to be deployed	1 s
7.	Activation of timer for explosive cutters	0.2 s
8.	Run time of timer to fire explosive cutters	0.2 s
9.	Velocity of test package when released from pallet	10 m/s
10.	Direction of test package when released	10°
11.	Altitude of test package when released relative to aircraft (velocity, direction, and altitude errors account only for uncertainties in the parachute trajectory calculations)	30 m
12.	Wind velocity	7 m/s
13.	Wind direction	30°
14.	Calculation of impact point (accounts for uncertainties in the method and data used in the package trajectory calculations)	100 m

### 3. PROBABILITY DISTRIBUTION OF TARGET MISS DISTANCE

#### 3.1 Method

We determine the probability distribution of  $D$ , the distance along the ground from the actual impact point to the target point. The location of the actual impact point relative to the target is characterized stochastically as an expression involving various random components. From assumed component probability distributions based on engineering judgment, the probability distributions of the actual impact location and of  $D$  are obtained by Monte Carlo simulation. A safe impact area can be determined by examining percentiles of the distribution of  $D$ .

We begin by defining a coordinate system based on perceived or measured conditions prior to the drop (see Fig. 4). The origin is the target. The  $(x, y)$ -plane is the ground plane, and the  $z$ -axis marks altitude. The  $x$ -axis is oriented to point into the perceived wind, which is assumed to be flowing from right to left. The aircraft is supposed to fly directly into the wind; therefore, ideally the aircraft heading is along the  $x$ -axis, from left to right. The point at which the drop sequence ideally is initiated is denoted by  $(x_{0i}, y_{0i}, z_{0i}) = (x_{0i}, 0, z_{0i})$ , where  $x_{0i}$  is calculated from relevant perceived conditions and modeled properties of the drop, and  $z_{0i}$  is the selected ideal altitude. We give below (see Eq. (28)) an expression for  $x_{0i}$  involving such factors as pilot reaction, aircraft speed, parachute performance, and package drop characteristics. The point at which the package ideally is released from the pallet and begins its drop free from the parachutes is denoted by  $(x_{1i}, y_{1i}, z_{1i}) = (x_{1i}, 0, z_{1i})$ , and the ideal impact point is  $(x_{2i}, y_{2i}, z_{2i}) = (0, 0, 0)$ , the target. We also give expressions (Eqs. 4 and 6) for  $x_{1i}$  and  $z_{1i}$ . The corresponding actual coordinates,  $(x_{0a}, y_{0a}, z_{0a})$  and  $(x_{1a}, y_{1a}, z_{1a})$ , and the actual impact point,  $(x_{2a}, y_{2a}, z_{2a}) = (x_{2a}, y_{2a}, 0)$ , are expressed in terms of their ideal counterparts and pertinent random factors.

The drop sequence is initiated when a signal is sent to the aircraft to release the pallet. At this time the aircraft is supposed to be located at  $(x_{0i}, 0, z_{0i})$ . However, due to pilot/equipment limitations, the actual position is  $(x_{0a}, y_{0a}, z_{0a})$ . The actual position may be modeled stochastically as:

$$z_{0a} = z_{0i} + \epsilon_z, \quad (1)$$

$$x_{0a} = x_{0i} + r_0 \cos \alpha, \quad (2)$$

$$y_{0a} = y_{0i} + r_0 \sin \alpha, \quad (3)$$

where  $\epsilon_z$ ,  $r_0$ , and  $\alpha$  are random variables with probability distributions to be selected according to engineering judgment. The variable  $\epsilon_z$  is the altitude error,  $r_0$  is the projected distance from  $(x_{0a}, y_{0a})$  to  $(x_{0i}, y_{0i})$ , and  $\alpha$  is the associated angle. Thus,



$(r_0, \alpha)$  denotes the polar coordinates of the actual drop sequence initiation point relative to the ideal, projected to the ground (see Fig. 5).

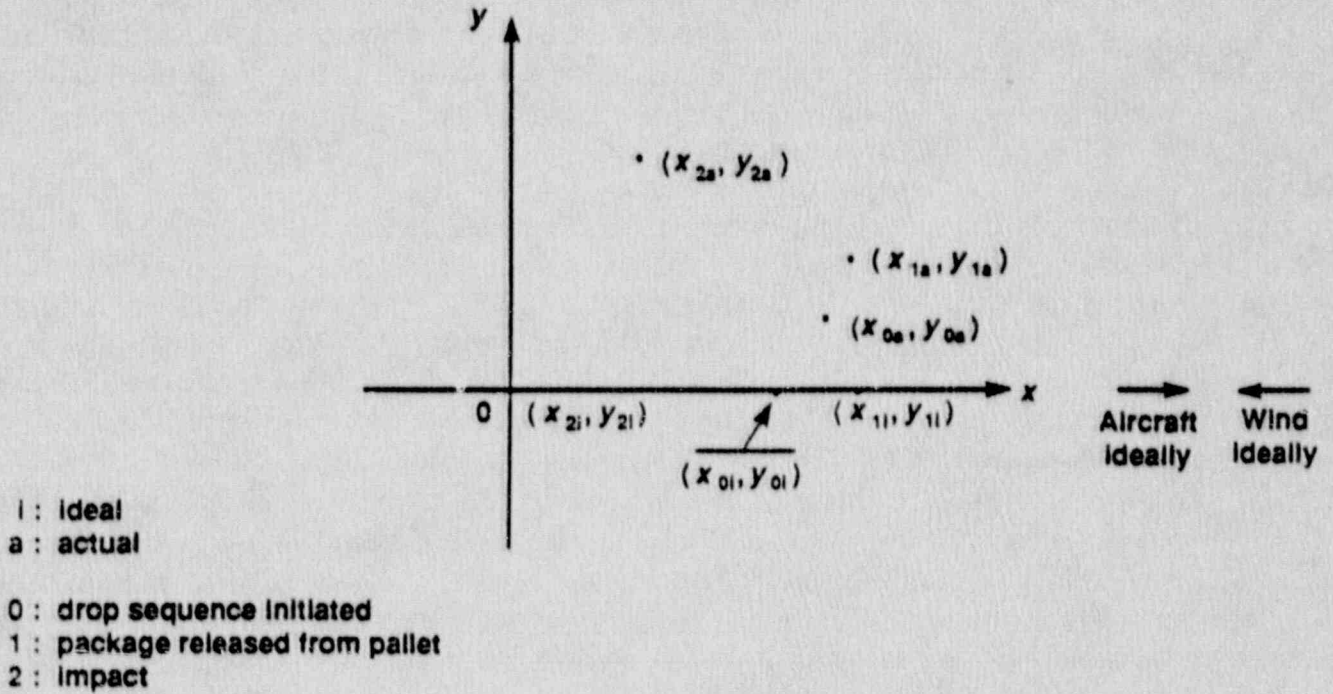


Fig. 4. The coordinate system used in this analysis.

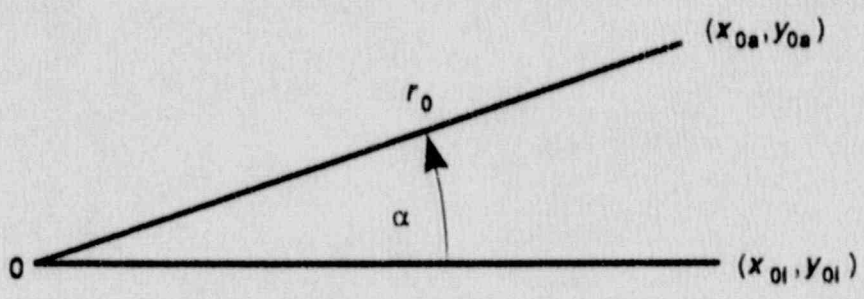


Fig. 5. Polar coordinates of actual initiation point of drop sequence relative to the ideal initiation point (both project-to-ground).

Consider now the time interval from initiation of the drop sequence to release of the package. We break this interval into three subintervals by defining four event times:

- (1) Signal sent to aircraft to release pallet.
- (2) Pilot/engineer presses button to release pallet.
- (3) Pallet/package exits aircraft as parachutes are deployed.
- (4) Package is released from pallet.

Ideally, projecting the position of the package to the ground, we have the situation shown in Fig. 6. The (projected) position at time (1) is  $(x_{0i}, 0)$ , and at time (4) it is  $(x_{1i}, 0)$ . Note that the position at time (4) is to the left of that at time (3) because of the combined effects of the parachutes and the wind. In fact, the ideal position at package release can be expressed in terms of known or hypothesized quantities:

$$x_{1i} = x_{0i} + t_{1i} r_i + t_{2i} (r_i - \rho_i) + d_i, \quad (4)$$

$$y_{1i} = 0, \quad (5)$$

$$z_{1i} = z_{0i} - \Delta z_i. \quad (6)$$

Here  $t_{1i}$  denotes the ideal length of the time interval between time (1) and time (2), i.e., the expected reaction time of the pilot/engineer;  $r_i$  denotes the ideal ground velocity of the aircraft;  $t_{2i}$  denotes the ideal length of the time interval between time (2) and time (3), i.e., the ideal length of time between pallet release and parachute deployment;  $\rho_i$  denotes the ideal average speed of the pallet relative to the aircraft during  $t_{2i}$  (the pallet is designed to slip backwards out the rear of the aircraft);  $d_i$  denotes the ideal horizontal displacement of the package during the parachute period from time (3) to time (4); and  $\Delta z_i$  denotes the ideal altitude loss of the package during this period.



Fig. 6. Ideal package position (projected to ground) at the four times (1), (2), (3), and (4).

The actual position at package release is determined by tracing the path of the package from time (1) to time (4). From time (1) to time (3) the package is inside the aircraft and therefore moves in the direction of the aircraft (see Fig. 7). Let the random variable  $\theta$  denote the actual heading angle of the aircraft, that is, relative to the ideal wind (the presumed wind direction). The distance moved by the package during this time period is:

$$d_{\theta} = t_{1a} r_a + t_{2a}(r_a - \rho_a). \quad (7)$$

Here  $t_{1a}$  denotes the actual length of the time interval between time (1) and time (2), i.e., the actual reaction time of the pilot/engineer;  $r_a$  denotes the actual ground velocity of the aircraft;  $t_{2a}$  denotes the actual length of time between time (2) and time (3); and  $\rho_a$  denotes the actual average speed of the pallet relative to the aircraft during  $t_{2a}$ . The random variables  $t_{1a}$ ,  $t_{2a}$ ,  $r_a$ , and  $\rho_a$  are modeled in terms of their ideal counterparts as:

$$t_{1a} = t_{1i} + \epsilon_1, \quad (8)$$

$$t_{2a} = t_{2i} + \epsilon_2, \quad (9)$$

$$r_a = r_i + \epsilon_r, \quad (10)$$

$$\rho_a = \rho_i + \epsilon_p, \quad (11)$$

where the error random variables  $\epsilon_1$ ,  $\epsilon_2$ ,  $\epsilon_r$ , and  $\epsilon_p$  have probability distributions to be selected according to engineering judgment.

The projected trajectory of the package/pallet in the parachute period from time (3) to time (4) is curved, as the combined influence of the parachutes and the wind change the direction of travel from the initial aircraft heading ultimately to the wind direction (see Fig. 7). The position at package release is obtained from the horizontal displacements of the package in the  $\theta$  and the perpendicular-to- $\theta$  directions. Key random variables involve the wind. Let the random variable  $\omega$  denote the actual angle of the wind relative to the ideal, or presumed, wind location. Define:

$$\delta = \omega - \theta, \quad (12)$$

the location of the actual wind relative to the actual heading of the aircraft. Denote the actual wind velocity by  $w_a$ . Then:

$$w_a = w_i + \epsilon_w, \quad (13)$$



where  $w_i$  denotes the ideal, or presumed, wind velocity, and the random variable  $\epsilon_w$  denotes the corresponding error. The component of wind velocity in the  $\theta$  direction is therefore  $w_a \cos \delta$ , and the component of wind velocity in the direction perpendicular to  $\theta$  is  $w_a \sin \delta$ .

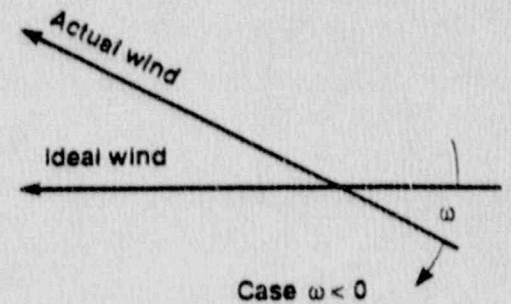
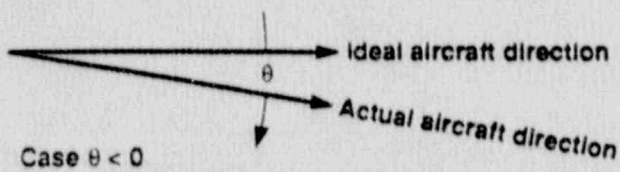
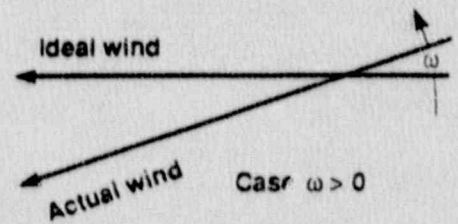
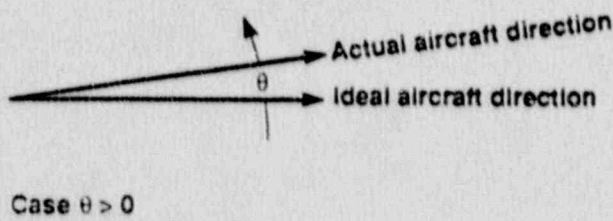
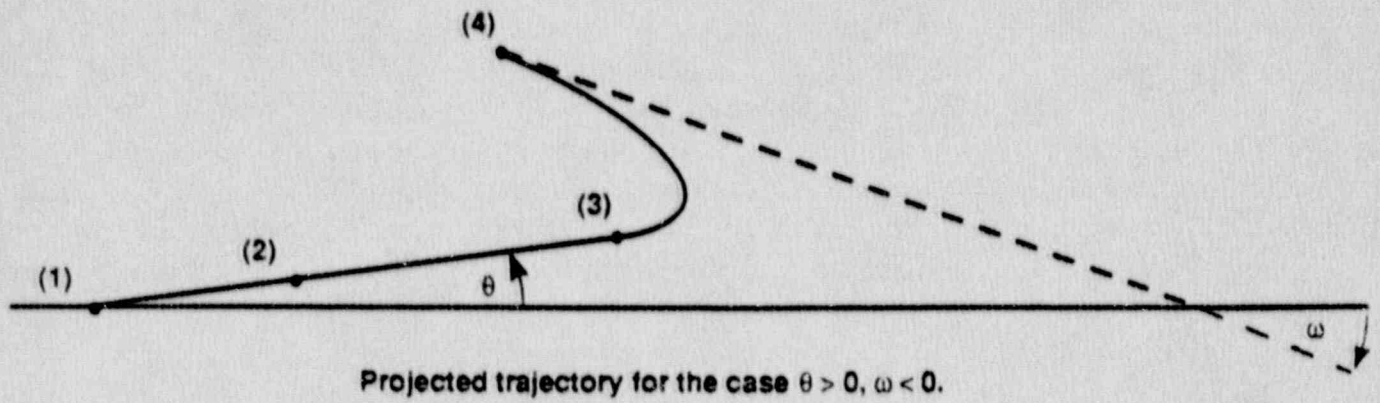


Fig. 7. Projected trajectory of the pallet/package assembly between the time a signal is given to initiate the drop and the time the package is released from the pallet. Also shown are defined errors  $\theta$  in aircraft heading and  $\omega$  in wind direction.

We now consider the horizontal displacement,  $c_\theta$ , of the package in the  $\theta$  direction during the parachute period. The actual length of time,  $t_{3a}$ , between time (3) and time (4) is related to the ideal parachute period length  $t_{3i}$  by the expression

$$t_{3a} = t_{3i} + \tau_1 + \tau_2, \quad (14)$$

where the independent random variables  $\tau_1$  and  $\tau_2$  characterize the two potential deviants in the timing mechanism responsible for firing the explosive cutters to release the package from the pallet:  $\tau_1$  denotes the error in activation of the timer, and  $\tau_2$  denotes the error in the length of the run time. Since the effect of the parachutes and the wind is to slow down and even reverse the direction of travel of the package, the average speed of the package during  $t_{3a}$  may differ greatly from the speed at package release. Hence it is expedient to break down the parachute period to obtain:

$$c_\theta = r_p t_{3i} + r_p^* (\tau_1 + \tau_2), \quad (15)$$

where  $r_p$  denotes the average horizontal speed in the  $\theta$  direction during  $t_{3i}$  and  $r_p^*$  denotes the horizontal speed in the  $\theta$  direction at package release.

To estimate  $r_p$ , we assume the average horizontal speed during  $t_{3i}$  is linear in wind speed:

$$r_p = a + b w_\theta + \epsilon_p, \quad (16)$$

where  $a$  and  $b$  are constants,  $w_\theta$  is the wind speed in the  $\theta$  direction, and  $\epsilon_p$  is the error random variable for this linear model. The constants  $a$  and  $b$  may be computed from known expected horizontal parachute period displacements for the ideal wind speed  $w_i$  (displacement =  $d_i$ ) and for zero wind speed (displacement =  $d_0$ ). Thus, for  $w_\theta = w_i$  we have  $E r_p = a + b w_i = d_i/t_{3i}$ , and for  $w_\theta = 0$  we have  $E r_p = a + b(0) = d_0/t_{3i}$ . Consequently,  $a = d_0/t_{3i}$  and  $b = (d_i - d_0)/(w_i t_{3i})$ . By substituting the actual component of wind velocity in the  $\theta$  direction, namely  $w_\theta = w_a \cos \delta$ , we have:

$$r_p t_{3i} = d_0/t_{3i} + [(d_i - d_0)/t_{3i}] (w_a/w_i) \cos \delta + \epsilon_p. \quad (17)$$

To estimate the horizontal speed,  $r_p^*$ , in the direction of  $\theta$  at package release, we consider the actual package velocity,  $v_a$ , at this time and the corresponding angle,  $\phi_a$ , relative to the horizon made by the package as it begins its descent free of the parachutes (see Fig. 8).

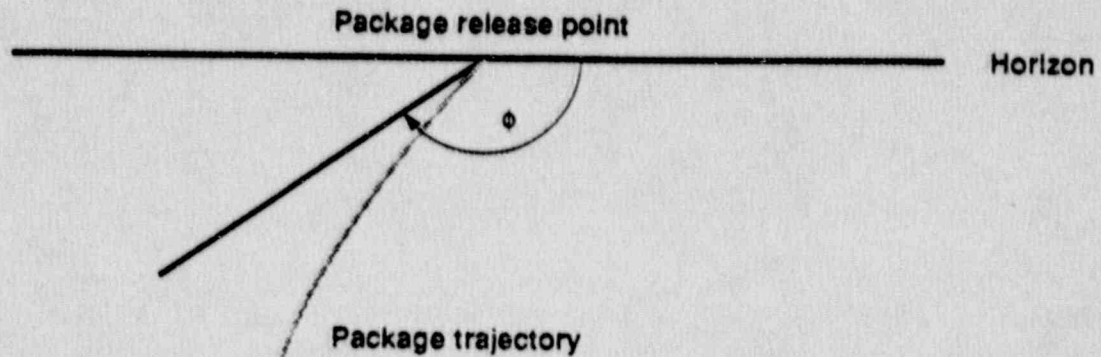


Fig. 8. Angle  $\phi$  to horizon at time of package release, and ensuing package trajectory.

We model the random variables  $v_a$  and  $\phi_a$  as:

$$v_a = v_i + \epsilon_v, \quad (18)$$

$$\phi_a = \phi_i + \epsilon_\phi, \quad (19)$$

where  $v_i$  and  $\phi_i$  denote the ideal, or presumed, counterparts, and  $\epsilon_v$  and  $\epsilon_\phi$  the associated random errors. The horizontal velocity of the package at package release is  $v_a \cos \phi_a$ , and assuming the parachute period is long enough so that by package release the horizontal component of movement is in approximately the wind direction, the horizontal speed in the  $\theta$  direction is:

$$r_p^* = v_a \cos \phi_a \cos \delta. \quad (20)$$

By combining (17) and (20) we obtain a useful expression for (15).

To estimate the parachute period horizontal displacement,  $c_\theta^*$ , perpendicular to the aircraft heading direction  $\theta$ , we must remove all effects of the aircraft's speed. Recall that  $d_i$  and  $d_0$  are the known expected horizontal displacements in the ideal parachute period of length  $t_{3i}$ , based on aircraft speed  $r_i$  and wind speed  $w_i$  and 0, respectively. Assuming a change in aircraft speed would affect  $d_i$  and  $d_0$  equally (e.g., reducing  $r_i$  by  $\Delta r$  would reduce both  $d_i$  and  $d_0$  by  $\Delta d$ ), it follows that  $d_i - d_0$  is the expected horizontal displacement if the aircraft speed is 0 and the wind speed is  $w_i$ . Since the component of aircraft speed in the direction perpendicular to the heading



is indeed 0, we have, assuming linearity, the expected horizontal displacement in  $t_{3i}$  perpendicular to  $q$  for wind speed  $w$  is  $(d_i - d_0) w/w_i$ . By imposing a random error proportional to wind speed in this relationship and correcting for the actual parachute period length, we obtain:

$$c_{\theta}^* = (d_i - d_0) (w_{\theta}^*/w_i) (t_{3a}/t_{3i}) (1 + \epsilon_c), \quad (21)$$

where  $w_{\theta}^* = w_a \sin \delta$  is the wind velocity in the direction perpendicular to  $\theta$ , and  $\epsilon_c$  is the error random variable embodying the wind proportionality effect.

The actual position at package release can now be determined from  $d_{\theta}$ , the horizontal displacement in the  $\theta$  direction in the preparachute period from time (1) to time (3),  $c_{\theta}$ , the horizontal displacement in the  $\theta$  direction in the parachute period, and  $c_{\theta}^*$ , the horizontal displacement perpendicular to  $\theta$  in the parachute period (see Fig. 9).

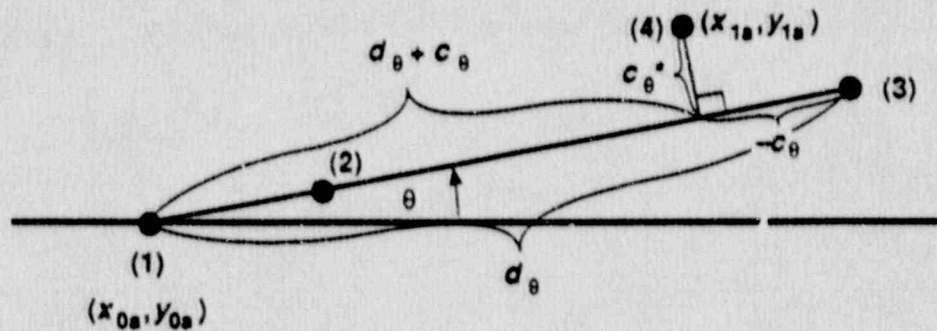


Fig. 9. Relationships for determining the actual position of the package (projected to ground) at package release.

Define  $\Delta x = x_{1a} - x_{0a}$  and  $\Delta y = y_{1a} - y_{0a}$ . The coordinates of (4) in the plane with origin (1) are  $(\Delta x, \Delta y)$ . Rotate this plane through angle  $\theta$ . The coordinates of (4) in this rotated plane are  $(d_{\theta} + c_{\theta}, c_{\theta}^*)$ . Thus:

$$\Delta x = (d_{\theta} + c_{\theta}) \cos \theta - c_{\theta}^* \sin \theta, \quad (22)$$

$$\Delta y = (d_{\theta} + c_{\theta}) \sin \theta + c_{\theta}^* \cos \theta, \quad (23)$$

and

$$x_{1a} = x_{0a} + (d_{\theta} + c_{\theta}) \cos \theta - c_{\theta}^* \sin \theta, \quad (24)$$

$$y_{1a} = y_{0a} + (d_{\theta} + c_{\theta}) \sin \theta + c_{\theta}^* \cos \theta. \quad (25)$$

Also, the actual altitude at package release,  $z_{1a}$ , is modeled as:

$$z_{1a} = z_{0a} - \Delta z_a, \quad (26)$$

where in turn  $\Delta z_a$ , the actual altitude loss for the period from time (1) to time (4), is related to the ideal altitude loss,  $\Delta z_i$ , by:

$$\Delta z_a = \Delta z_i + \epsilon_g, \quad (27)$$

with  $\epsilon_g$  being a random variable with a probability distribution selected according to engineering judgment.

The package trajectory from package release to impact is modeled by a ballistics computer code that was developed to produce the data presented in Ref. 2. The expected, or predicted, horizontal displacement from package release to impact is a function of five variables,  $h(z, v_h, v_v, w, q)$ , where:

- $z$  = altitude at package release,
- $v_h$  = horizontal velocity at package release,
- $v_v$  = downward vertical velocity at package release,
- $w$  = wind velocity during fall,
- $q$  = index of the tumbling action of the package during the fall.

The model assumes the package moves horizontally in either an upwind or downwind direction while falling to the ground. In the ideal situation, the aircraft flies directly into the wind (upwind); however, the effect of the wind and parachutes is to reverse the direction of the package so that  $v_{hi} < 0$  ( $v_{hi}$  denotes the ideal horizontal velocity at package release), and the package moves in the downwind direction as it falls to the ground. In the actual situation, the aircraft flies approximately into the wind, yet by the time of package release, the parachutes and wind have caused the package to be moving in the downwind direction, with  $v_{ha} < 0$  ( $v_{ha}$  denotes the actual horizontal velocity at package release). The tumbling index  $q$  reflects the behavior of the package as it tumbles to the ground. The actual index  $q_a$  will be somewhere between a wholly axial mode and a wholly side mode. Ideally, a combination of axial and side motions is expected. The index to describe the ideal tumbling behavior is defined to be  $q_i = 1$ .

The ideal horizontal displacement  $h_i = h(z_i, v_{hi}, v_{vi}, w_i, q_i)$  is computed from the ballistics code for the ideal inputs:

$$z_i = z_{1i}, \quad v_{hi} = v_i \cos \phi_i, \quad v_{vi} = v_i \sin \phi_i, \quad w_i = w_i, \quad \text{and} \quad q_i = 1.$$

In order to predict impact at the target, the ideal horizontal position at package release,  $(x_{1i}, 0)$ , must be  $(-h_i, 0)$ . (Note that  $h_i < 0$  because the wind speed  $w_i$  is



negativ<sup>e</sup>) Consequently, we have determined the ideal position,  $x_{0i}$ , of the aircraft at initiation of the drop sequence. From Eq. (4) and  $x_{1i} = -h_i$ , it follows that:

$$x_{0i} = -[h_i + t_{1i} r_i + t_{2i}(r_i - \rho_i) + d_i]. \quad (28)$$

The ideal horizontal displacement  $h_i$  is the expected displacement using the ballistics computer model for the ideal inputs ( $z_i, v_{hi}, v_{vi}, w_i, q_i$ ). There will be deviations from this ideal in the actual fall due to three major factors. First, because of theoretical simplifications, there is an unknown bias in the ballistics code. The true mean horizontal displacement is

$$h_t = h_i + B, \quad (29)$$

where  $B$  is the ballistics model bias. Although  $B$  is necessarily unknown (otherwise it would be corrected for), a conservative (i.e., large) value will be postulated in subsequent computational assessments (see Section 3.2). A second source of deviation is the disparity between the actual inputs ( $z_a, v_{ha}, v_{va}, w_a, q_a$ ) and the ideal inputs. A first order approximation with differentials will be used to address this problem. The third source of deviation is the random variation of the actual displacement from its expectation.

Because of the model bias,  $B$ , the expected impact point in the ideal-inputs situation is not the target  $(0, 0)$ , but rather  $(B, 0)$ , since impact on the average would occur at  $x_{1i} + h_t = -h_i + h_i + B = B$ . Thus, the coincidence of the target  $(0, 0)$  and ideal impact point  $(x_{2i}, y_{2i})$  in Fig. 4 represents the optimistic no-bias ( $B = 0$ ) case.

The actual impact point  $(x_{2a}, y_{2a})$  is estimated by projecting the package to move from the actual package release point  $(x_{1a}, y_{1a})$  in the downwind direction a horizontal distance equal to:

$$h_a = B + h^*(z_a, v_{ha}, v_{va}, w_a, q_a) + \epsilon_\Delta + \epsilon_m. \quad (30)$$

Here  $h^*$  denotes the first order approximation of  $h$  to be described below,  $z_a = z_{1a}$ ,  $v_{ha} = v_a \cos \phi_a$ ,  $v_{va} = v_a \sin \phi_a$ ,  $w_a = w_a$ ,  $q_a = q_a$  are the actual inputs,  $\epsilon_\Delta$  denotes the error random variable for this approximation (reflecting the accuracy of the approximation), and  $\epsilon_m$  denotes the error random variable, which is the difference between the actual horizontal displacement and its mean. The approximation function  $h^*$  is defined as:

$$h^*(z_a, v_{ha}, v_{va}, w_a, q_a) = h_i + (\partial h / \partial z)_i \Delta z + (\partial h / \partial v_h)_i \Delta v_h + (\partial h / \partial v_v)_i \Delta v_v \\ + (\partial h / \partial w)_i \Delta w + (\partial h / \partial q)_i \Delta q, \quad (31)$$



where:

$$\Delta z = z_a - z_i = z_{1a} - z_{1i} = \epsilon_z - \epsilon_g,$$

$$\Delta v_h = v_{ha} - v_{hi} = v_a \cos \phi_a - v_i \cos \phi_i = (v_i + \epsilon_v) \cos (\phi_i + \epsilon_\phi) - v_i \cos \phi_i,$$

$$\Delta v_v = v_{va} - v_{vi} = v_a \sin \phi_a - v_i \sin \phi_i = (v_i + \epsilon_v) \sin (\phi_i + \epsilon_\phi) - v_i \sin \phi_i,$$

$$\Delta w = w_a - w_i = \epsilon_w, \text{ and}$$

$$\Delta q = q_a - q_i = \epsilon_q.$$

(Here  $q_a = q_i + \epsilon_q$ , with  $\epsilon_q$  being the error random variable describing the difference between actual and ideal tumbling actions.) Thus  $h^*$  is the first-order Taylor series approximation about  $(z_i, v_{hi}, v_{vi}, w_i, q_i)$ . Approximate values of the derivatives are obtainable from experimental results. (See Section 3.2 for details.)

Since the horizontal displacement of the package from package release  $(x_{1a}, y_{1a})$  to impact  $(x_{2a}, y_{2a})$  is the amount  $h_a$  along the angle  $w$  (see Fig. 10), we have:

$$x_{2a} = x_{1a} + h_a \cos \omega, \tag{32}$$

$$y_{2a} = y_{1a} + h_a \sin \omega. \tag{33}$$

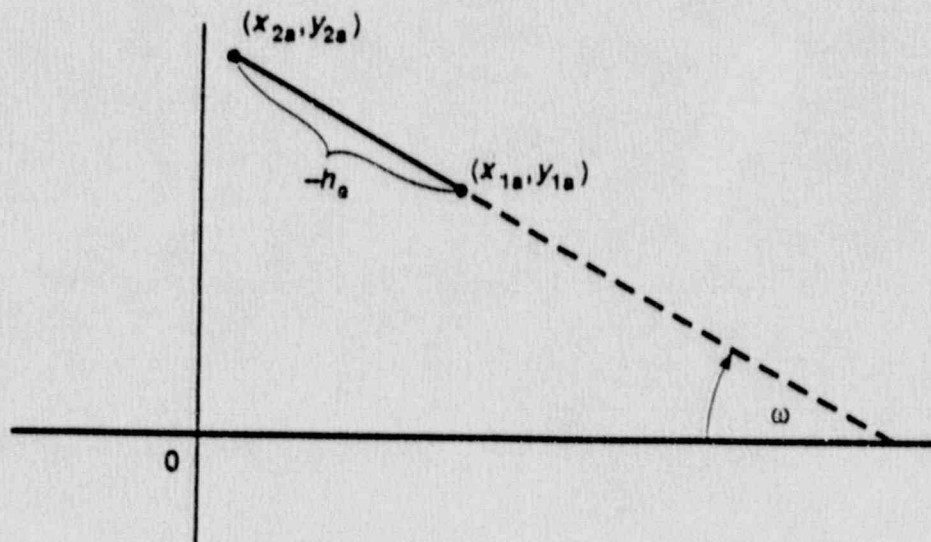


Fig. 10. Relationships for determining the actual position of the package at ground impact.

The distance from the actual impact point to the target is therefore:

$$D = [(x_{2a})^2 + (y_{2a})^2]^{1/2}. \quad (34)$$

The impact coordinates may be expressed in terms of the error variables and constants involved in the development. In summary, by combining results Eq. (1) to Eq. (33), we obtain:

$$x_{2a} = -[h_i + t_{1i} r_i + t_{2i}(r_i - \rho_i) + d_i] + r_0 \cos \alpha \\ + A \cos \theta - c_{\theta}^* \sin \theta + h_a \cos \omega, \quad (35)$$

$$y_{2a} = r_0 \sin \alpha + A \sin \theta + c_{\theta}^* \cos \theta + h_a \sin \omega, \quad (36)$$

where:

$$A = (t_{1i} + \epsilon_1) (r_i + \epsilon_r) + (t_{2i} + \epsilon_2) (r_i + \epsilon_r - \rho_i - \epsilon_r) + d_0/t_{3i} \\ + [(d_i - d_0)/t_{3i}] [(w_i + \epsilon_w)/w_i] \cos (\omega - \theta) + \epsilon_p \\ + (\tau_1 + \tau_2) (v_i + \epsilon_v) \cos (\phi_i + \epsilon_\phi) \cos (\omega - \theta), \quad (37)$$

$$c_{\theta}^* = (d_i - d_0) [(w_i + \epsilon_w)/w_i] [(t_{3i} + \tau_1 + \tau_2)/t_{3i}] (1 + \epsilon_c) \sin (\omega - \theta), \quad (38)$$

$$h_a = B + \epsilon_\Delta + \epsilon_m + h_i + (\partial h/\partial z)_i (\epsilon_z - \epsilon_g) \\ + (\partial h/\partial v_h)_i [(v_i + \epsilon_v) \cos (\phi_i + \epsilon_\phi) - v_i \cos \phi_i] \\ + (\partial h/\partial v_v)_i [(v_i + \epsilon_v) \sin (\phi_i + \epsilon_\phi) - v_i \sin \phi_i] + (\partial h/\partial w)_i \epsilon_w + (\partial h/\partial q)_i \epsilon_q. \quad (39)$$

The quantities  $h_i, t_{1i}, t_{2i}, t_{3i}, r_i, \rho_i, d_i, d_0, w_i, v_i, \phi_i, B, (\partial h/\partial z)_i, (\partial h/\partial v_h)_i, (\partial h/\partial v_v)_i, (\partial h/\partial w)_i,$  and  $(\partial h/\partial q)_i$  are known or postulated constants, whereas  $r_0, a, \theta, \omega, \epsilon_1, \epsilon_2, \epsilon_r, \epsilon_\rho, \epsilon_w, \epsilon_p, \tau_1, \tau_2, \epsilon_v, \epsilon_\phi, \epsilon_c, \epsilon_\Delta, \epsilon_m, \epsilon_z, \epsilon_g,$  and  $\epsilon_q$  are error random variables. By using engineering judgment to specify completely each random variable, the probability distribution of the impact location  $(x_{2a}, y_{2a})$  and of the distance  $D$  to the target can be determined by Monte Carlo simulation according to Section 3.2, which follows.

### 3.2 Results

The results of the previous Section, which characterize the impact location and  $D$  in terms of postulated constants and random errors, are used to evaluate, for various scenarios, the probability distribution of the distance  $D$  from the impact point to the

target. For each complete specification of all the random error probability distributions, a scenario is created. The impact location and  $D$  are generated repeatedly in Monte Carlo simulations for each scenario to provide a scatter plot of impacts and the empirical distribution function of  $D$ . By varying parameters of the error variables, we are able to identify the major contributors to target misses as well as to portray the sensitivity of the distance distribution to these parameter values.

Two types of error distributions were used in the Monte Carlo simulations. The first (see Fig. 11) was a uniform, or rectangular, distribution over the interval  $[-c, c]$ . The probability density function for an error variable  $U$  with this distribution is constant over the range  $[-c, c]$  so that the probability for any subinterval is proportional to the length of the subinterval. Thus by assumption it is as likely that the error will fall between  $-c$  and  $-c + \epsilon$  as between  $-\epsilon/2$  and  $\epsilon/2$ . For a given error variable, the constant  $c$  is the upper bound on the absolute error; i.e.,  $|U| \leq c$  with a probability of one.

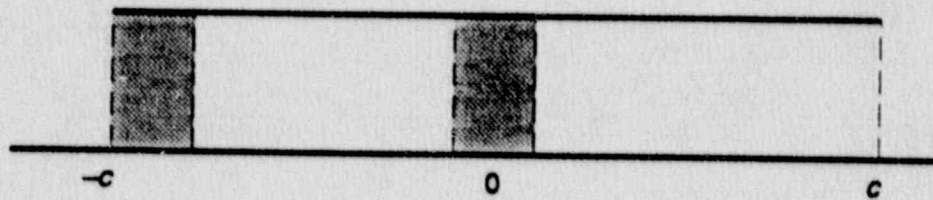


Fig. 11. Uniform error distribution used in the calculations.

The second error distribution we used in simulations was a triangular distribution (Fig. 12) with 95% of its probability contained in the interval  $[-c, c]$ . The probability density function for an error random variable  $T$  with this distribution is an isosceles triangle about 0 with end points  $\pm d$ , where  $d = c[(20 + 2\sqrt{5})/19] = 1.288 c$ . Although both uniform and triangular error distributions are symmetric about 0 and have means of 0 (so that errors average out to zero, and negative-valued errors are as likely as positive-valued errors), triangular errors are more concentrated about 0. However, since  $d > c$ , triangular errors can be larger than their uniform counterparts. The constants  $c$  were selected for each error variable according to engineering judgment. The Monte Carlo simulations generally use either all uniform or all triangular error distributions for the variable considered. An exception to this is the variable,  $\alpha$ , which is assumed to always have a uniform distribution.



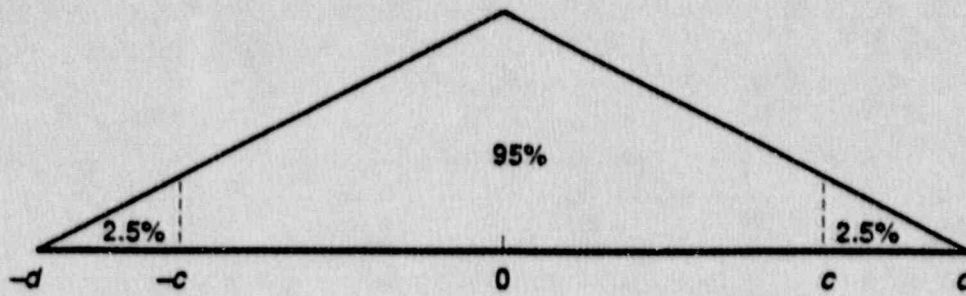


Fig. 12. Triangular error distribution used in the calculations.

In Table 3, a list of the constants used in the simulations is presented, and in Table 4 the error variables are presented with corresponding parameters  $c$ . (These tables are similar to Tables 1 and 2, respectively.) All constants and parameters displayed reflect conservative engineering judgment. Refer to Section 3.1 for elaboration on the meaning of these constants and variables. The constants  $z_{0i}$  and  $\Delta z_i$ , which involve the altitude of the package, are not used explicitly in the distributions for  $D$ . However, these constants are implicit factors in the determination of the ideal horizontal displacement,  $h_i$ , and of the derivative  $(\partial h / \partial z)_i$ . We estimated the derivatives in the Taylor approximation from various plots of predictions based on the ballistic code. Refer to Fig. 13, which plots altitude of the package versus horizontal position for selected horizontal release velocities. For  $v_h = 10$  m/s, we have  $\Delta h / \Delta z = -0.05$ , and for  $v_h = 50$  m/s, we have  $\Delta h / \Delta z = -0.2$ . Assuming linearity, we obtain for  $v_{hi} = v_i \cos \theta_i = 21.2$  m/s,

$$\Delta h / \Delta z = -0.05 + [(-0.2 + 0.05) / (50 - 10)] (21.2 - 10) = -0.09. \quad (40)$$

Also from this figure we estimate  $(\partial h / \partial v_h)_i$ . For  $v_h = 10$  m/s we have  $h = 450$  m, and for  $v_h = 50$  m/s we have  $h = 2100$  m. Thus we obtain:

$$\Delta h / \Delta v_h = (2100 - 450) / (50 - 10) \text{ sec} = 41 \text{ sec}. \quad (41)$$

For  $(\partial h / \partial v_v)_i$  we use Fig. 14, which plots altitude versus free-fall velocity. At release it is seen that  $\Delta z = -200$  m for  $\Delta v_v = 50$  m/s. Consequently,

$$\Delta h / \Delta v_v = (\Delta h / \Delta z) (\Delta z / \Delta v_v) = -0.09 (-200 / 50) \text{ sec} = 0.36 \text{ sec}. \quad (42)$$

Table 3. List of constants.

Constant	Value	Meaning
$t_{1i}$	0.5 s	Ideal, or expected, time from signal to release pallet to actual release.
$t_{2i}$	3.0 s	Ideal time from pallet release to parachute deployment.
$t_{3i}$	18.0 s	Ideal time from parachute deployment to package release.
$r_i$	77.3 m/s	Ideal aircraft ground velocity.
$\rho_i$	1.0 m/s	Ideal average speed of pallet relative to aircraft during $t_{2i}$ .
$z_{0i}$	7620 m	Ideal aircraft altitude.
$w_i$	-22.2 m/s	Ideal wind velocity at $z_{0i}$ .
$\Delta z_i$	610 m	Ideal altitude loss of package during $t_{3i}$ .
$d_i$	-85 m	Ideal horizontal displacement of package during $t_{3i}$ (wind = $w_i$ ).
$d_0$	300 m	Expected horizontal displacement of package during $t_{3i}$ (no wind).
$v_i$	46.7 m/s	Ideal velocity of package at package release.
$\phi_i$	117°	Ideal angle of package velocity vector at package release relative to horizontal velocity vector of drop aircraft.
$h_i$	-894 m	Ideal horizontal displacement from package release to impact point.
$B$	100 m	LLNL model bias for $h_i$ .
$(\partial h / \partial z)_i$	-0.09	Ideal rate of change of horizontal displacement versus altitude.
$(\partial h / \partial v_h)_i$	41 s	Ideal rate of change of horizontal displacement versus horizontal package velocity.
$(\partial h / \partial v_v)_i$	0.36 s	Ideal rate of change of horizontal displacement versus downward vertical package velocity.
$(\partial h / \partial w)_i$	42 s	Ideal rate of change of horizontal displacement versus wind velocity.
$(\partial h / \partial q)_i$	1.0 m	Ideal rate of change of horizontal displacement versus tumbling index.

Table 4. List of error random variables.

Variable	Parameter, $c$	Meaning
$(r_0, \alpha)$	$(60 \text{ m}, 180^\circ)^a$	$(r_0, \alpha)$ are polar coordinates of actual position of aircraft (projected to ground), relative to ideal position, at signal to release pallet.
$\epsilon_z$	30 m	Actual aircraft altitude relative to ideal altitude.
$\theta$	$0.5^\circ$	Actual heading angle of aircraft relative to ideal angle.
$\omega$	$30^\circ$	Actual direction of wind relative to ideal wind direction.
$\epsilon_1$	0.25 s	Actual time from signal to release pallet to pallet release, relative to ideal time.
$\epsilon_2$	1.0 s	Actual time from pallet release to parachute deployment, relative to ideal time.
$\tau_1$	0.2 s	Error in activation of timer for explosive cutters.
$\tau_2$	0.2 s	Error in length of run-time of timer for explosive cutters.
$\epsilon_T$	5.0 m/s	Actual ground velocity of aircraft relative to ideal velocity.
$\epsilon_p$	0.5 m/s	Actual average speed of pallet relative to aircraft, relative to ideal speed.
$\epsilon_w$	7.0 m/s	Actual wind velocity relative to ideal wind velocity.
$\epsilon_p$	1.0 m/s	Error variable in linear model for average horizontal speed in $\theta$ direction (parachute period).
$\epsilon_v$	10 m/s	Actual package velocity at package release, relative to ideal velocity.
$\epsilon_\phi$	$10^\circ$	Actual angle of package velocity vector with respect to aircraft horizontal velocity vector at package release, relative to ideal angle.
$\epsilon_c$	0.2	Wind proportionality effect for horizontal displacement perpendicular to $\theta$ (parachute period).
$\epsilon_B$	30 m	Actual altitude loss of package relative to ideal (parachute period).
$\epsilon_\Delta$	10 m	Error in using Taylor approximation for horizontal displacement from package release to impact.
$\epsilon_m$	25 m	Actual horizontal displacement, relative to expected displacement, from package release to impact.
$\epsilon_d$	5	Actual tumbling index relative to ideal tumbling index.

a Since  $r_0$ , a distance, is necessarily positive-valued, it is modeled as  $|U|$  or  $|T|$ , where  $U$  and  $T$  are uniform and triangular distributions, respectively, with parameter  $c = 60 \text{ m}$ . Regardless of the distribution of  $r_0$ ,  $\alpha$  is modeled as uniform over the interval  $[-180^\circ, 180^\circ]$ , or equivalent,  $[0^\circ, 360^\circ]$ .



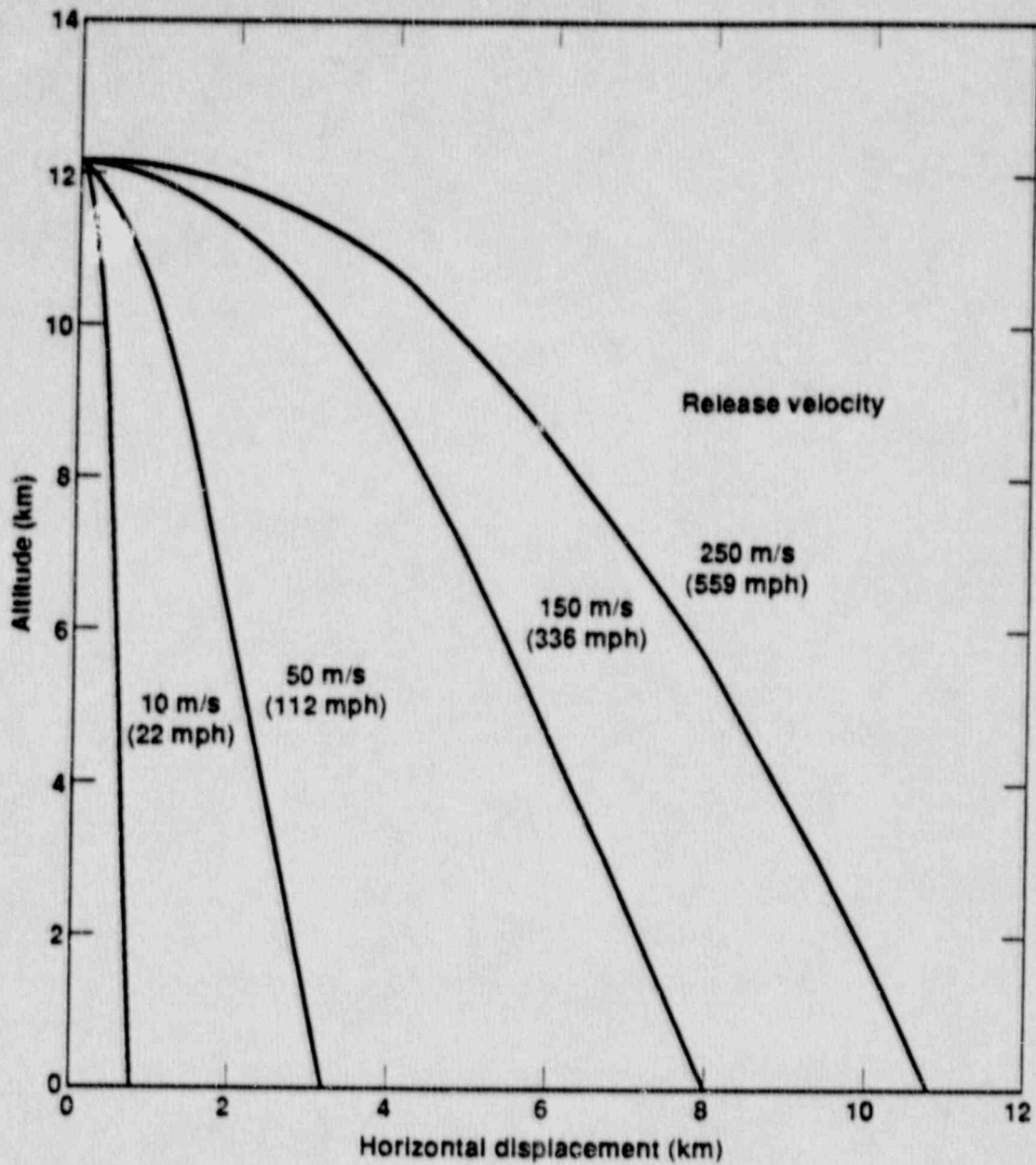


Fig. 13. Calculated trajectories of example PAT test package released from 12.2 km at selected release velocities (Ref. 2).

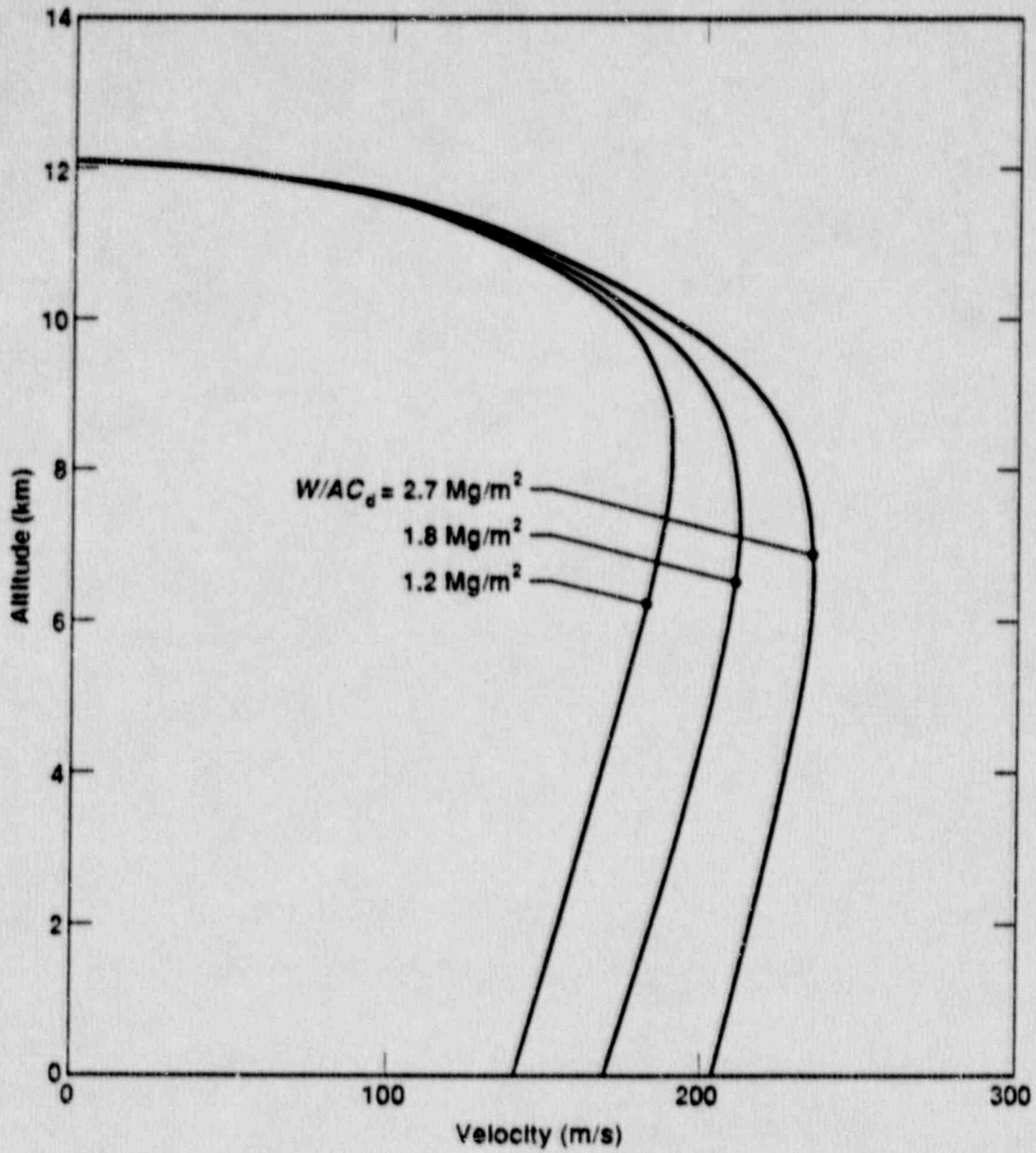


Fig. 14. Calculated free-fall velocities of three different packages released at 12.2 km;  $W$  = package weight, Mg;  $A$  = aerodynamic frontal area,  $\text{m}^2$ ;  $C_d$  = aerodynamic drag coefficient (Ref. 2).

We estimate  $(\partial h / \partial w)_i$  from Fig. 3, which plots altitude versus horizontal position for the assumed standard wind,  $w_i = -22.2$  m/s, and for no wind. From  $(h_i, w_i) = (-894, -22.2)$  and  $(h_0, w_0) = (45, 0)$ , we obtain:

$$\Delta h / \Delta w = (-894 - 45) / (-22.2 - 0) \text{ sec} = 42 \text{ sec.} \quad (43)$$

Finally, we define the tumbling index derivative to be  $(\partial h / \partial q)_i = 1.0$  m, so that the contribution,  $(\partial h / \partial q)_i \Delta q = \epsilon_q$  meters, in the approximation for actual horizontal displacement, represents the random horizontal displacement discrepancy, in meters, due to the actual tumbling action deviating from the ideal. Referring to Fig. 15, which plots altitude versus horizontal displacement for purely axial and purely side orientation modes, we assume the ideal tumbling action to be something between these two extremes. We determined the difference in horizontal displacements between the side and axial modes, after a 7000-m drop, from this plot to be 100 m for a horizontal release velocity of 225 m/s. Under the assumption of linearity, this difference would be  $(21.2/225)(100 \text{ m}) = 10$  m for the ideal release velocity. Thus, the tumbling action random variable  $\epsilon_q$  has the parameter  $c = 5$  to provide a distribution of tumbling effects over the interval  $[-5, 5]$  of length 10.

The only random variables in Table 4 which are not modeled as  $U$  or  $T$  with parameter  $c$  are the horizontal polar coordinates,  $(r_0, \alpha)$ , of the aircraft, relative to the ideal horizontal location, at the signal to release the pallet. Since  $r_0$  is a distance and cannot be negative, it is reasonable to model  $r_0$  as  $|U|$  or  $|T|$ . Further, since the angle  $\alpha$  can be any value in  $[0^\circ, 360^\circ]$  with equal likelihood, it is reasonable to model  $\alpha$  as uniform over this interval.

Table 5 shows the results of Monte Carlo simulations based on the modeling of Section 3.1 and the constants and parameters of Tables 3 and 4. "Nominal triangular" refers to the use of the triangular error component models with the parameter values of Table 4. "Nominal uniform" likewise refers to the corresponding uniform error component models. We simulated 50,000 drop sequences for each nominal scenario, resulting in 50,000 simulated impact points,  $(x_{2a}, y_{2a})$ , and 50,000 distances to the target,  $D$ . The average distance (e.g., 413 m for the triangular model) is the average of the 50,000 simulated distances, and it is an estimate of the expected (mean) distance from the impact point to the target. The standard deviation of distance (e.g., 198 m for the triangular model) is the sample standard deviation of the 50,000 simulated distances, and it is an estimate of the true standard deviation of the random distance  $D$ . The distance percentiles are obtained from the ordered simulated distances. For example, the 90th percentile for the triangular model is 681 m, which means the  $0.90(50,000) = 45,000$ th shortest distance among the 50,000 is 681 m. We then estimate the probability that the distance  $D$  would be 681 m or less to be 0.90, if the stated assumptions (involving the modeling in Section 3.1 and the constants and parameters of Tables 3 and 4) are valid.



Conversely, we estimate the probability of the distance exceeding 681 m to be 0.10. A "safe" impact area might be defined as a circle centered at the target with radius equal to the 99th percentile of distance. For such an area, the probability that the point of impact would fall outside is only 0.01, provided the stated assumptions are valid. Figure 16 shows a curve of the miss distance distribution for nominal triangular components. Scatter plots of 10,000 simulated impacts are given in Figs. 17 and 18 for the nominal triangular and uniform cases, respectively. Note the symmetry with respect to the  $x$ -axis but not the  $y$ -axis. There is  $x$ -axis symmetry because of symmetry in the error component distributions for location of the aircraft, heading direction, and wind direction. There is a cone-shaped asymmetry relative to the  $y$ -axis due to the effect of the wind coming from the right and the package continuing in the direction of the wind once it is released from the pallet.

Tables 6 and 7 show the sensitivity of the miss distance distribution to changes in assumed parameter values, for the triangular and uniform scenarios, respectively. In cases (a) through (g), one or two selected parameters are altered from their nominal values, while the remaining parameter values are left unaltered. Other cases of single departures from the nominal are not reported in the tables because their distance distributions are not significantly different from the nominal. Cases (h) and (i) represent all parameters, including the model bias  $B$ , being halved and doubled, respectively. The results given for each case (a) through (i) are based on 10,000 simulated drop sequences. It is apparent from Tables 6 and 7 that the wind direction and wind velocity errors—see cases (a), (b), and (c)—are the most important contributors to target misses.

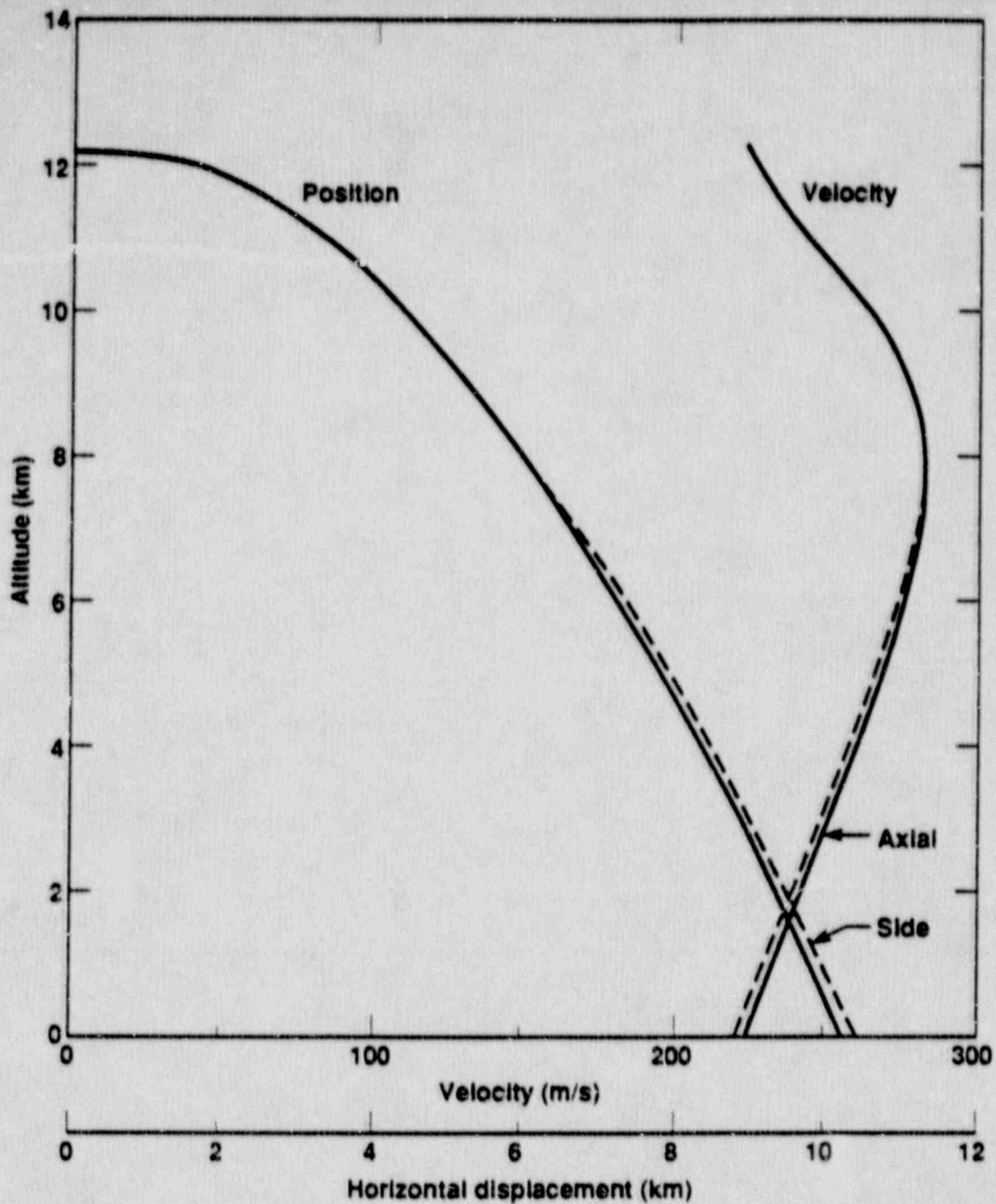


Fig. 15. Calculated trajectory and free-fall velocity of the example PAT test package released at 12.2 km with 225 m/s (434 knots) horizontal velocity. Side and axial orientations are relative to the fall direction (Ref. 2).

Table 5. Miss distance distribution for nominal triangular and nominal uniform components.

<u>Percentile</u>	<u>Miss distance (m)</u>	
	<u>Triangular</u>	<u>Uniform</u>
1	49	62
5	110	137
10	157	196
20	229	284
30	290	354
40	347	415
50	402	471
60	459	525
70	522	576
80	591	628
90	681	699
95	750	764
99	881	885
Average miss distance	413	461
Standard deviation	198	191
Maximum miss distance in 50,000 drops	1260	1140

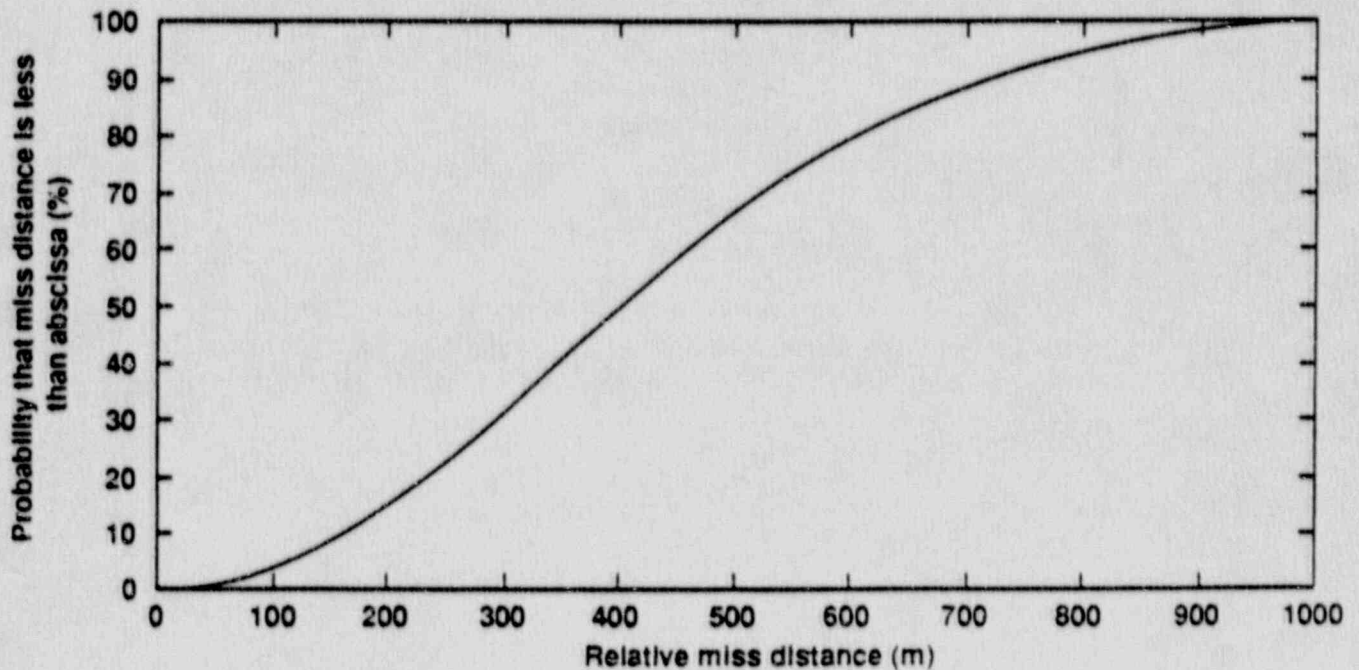


Fig. 16. Calculated probability as a function of miss distance for nominal triangular components.



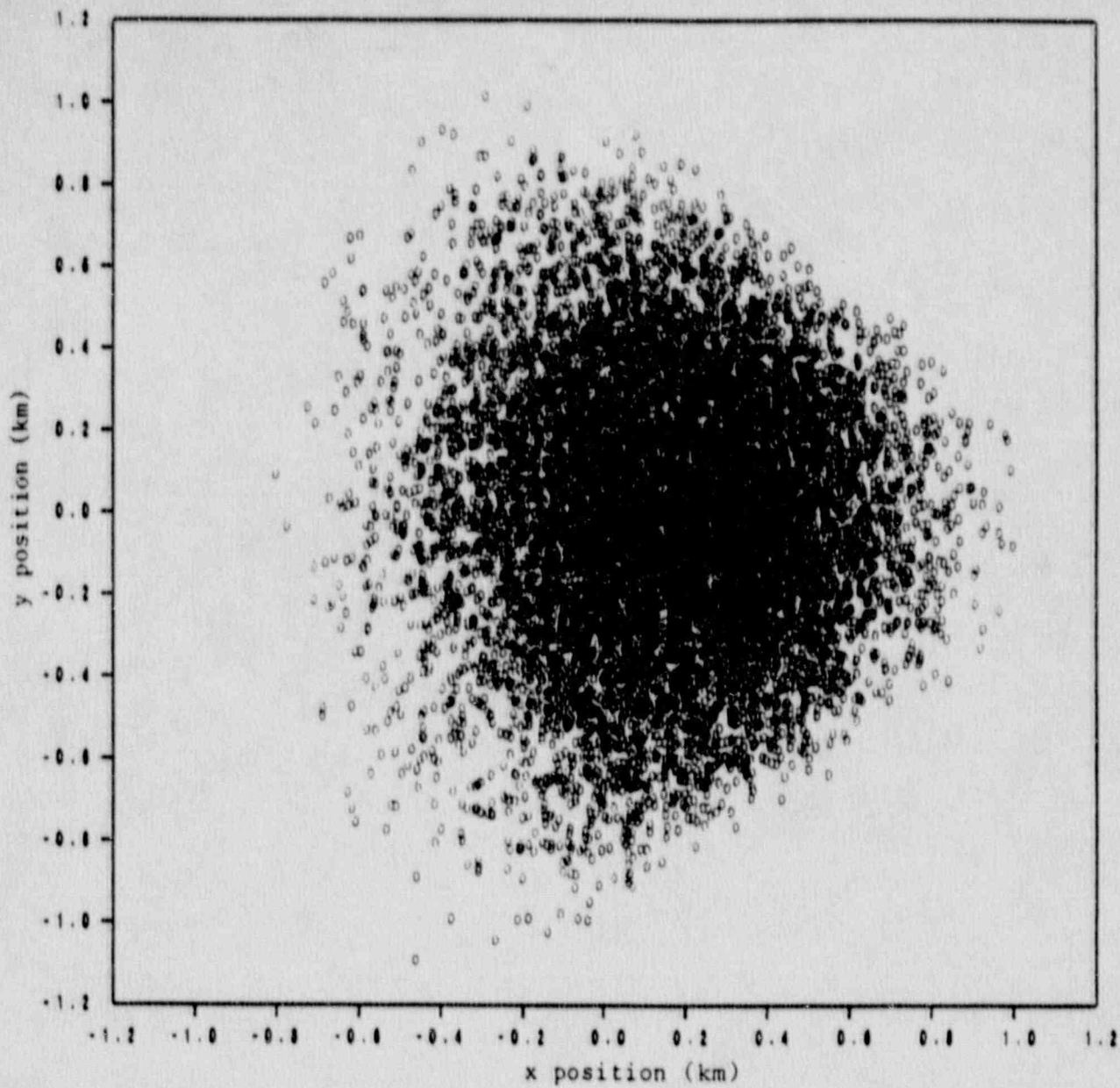


Fig. 17. Calculated impact positions of 10,000 simulated drops for the nominal triangular case.

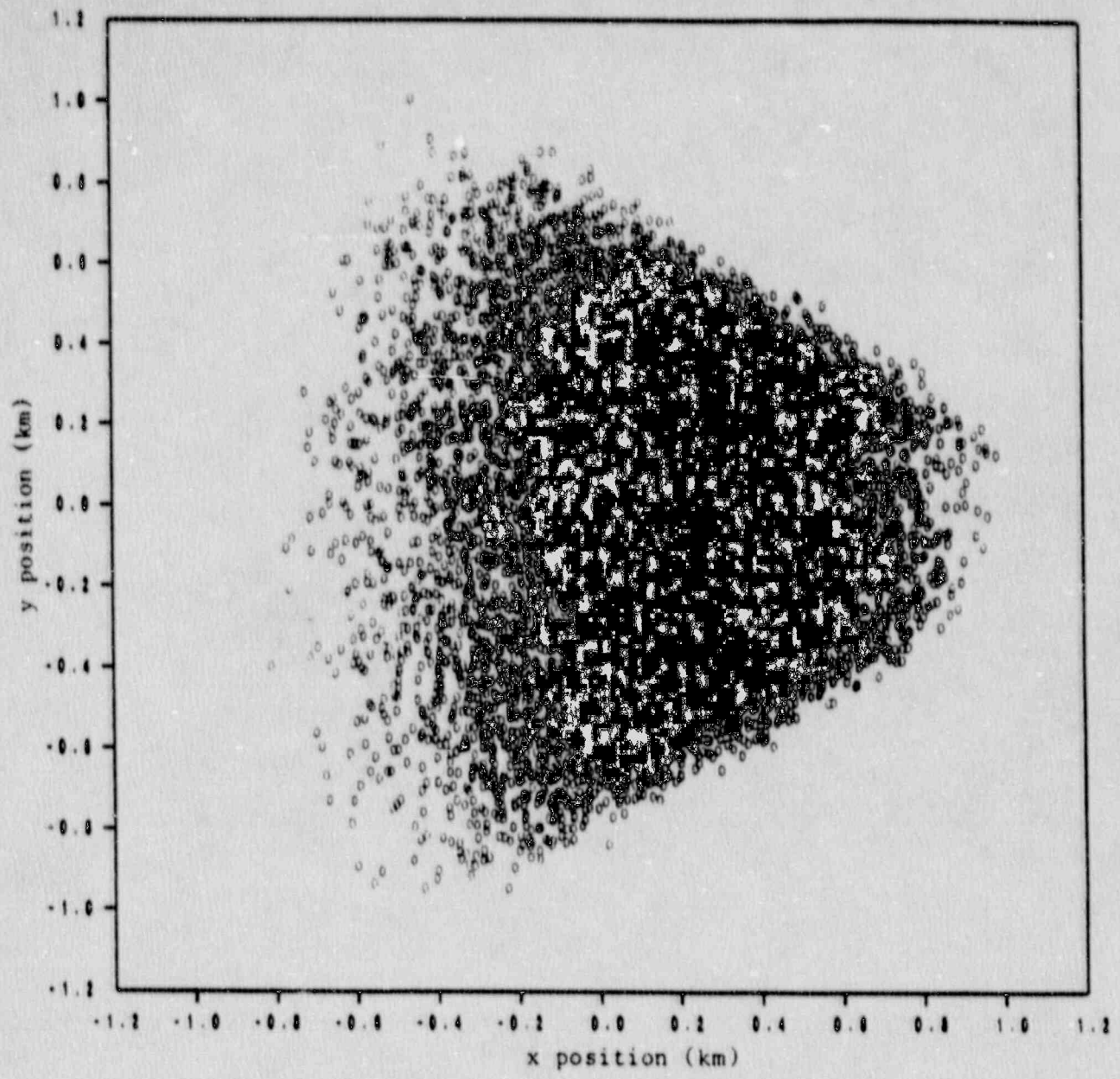


Fig. 18. Calculated impact positions of 10,000 simulated drops for the nominal uniform case.

Table 6. Miss distance distribution for triangular components and selected departures from the nominal case.

	Miss distance (m) for nominal case and departures from it									
	Nominal	(a)	(b)	(c)	(d)	(e)	(f)	(g)	(h)	(i)
Average	413	287	370	234	390	403	385	425	208	795
90th percentile	681	528	625	411	647	670	642	686	345	1280
95th percentile	750	613	690	473	716	735	707	758	380	1440
99th percentile	881	767	797	586	831	858	810	908	438	1760

Key to departures from nominal case:

- (a) Wind direction,  $\omega$  ( $c = 10^\circ$ ).
- (b) Wind velocity,  $\epsilon_w$  ( $c = 3.0$  m/s).
- (c) Wind direction,  $\omega$  ( $c = 10^\circ$ ); wind velocity,  $\epsilon_w$  ( $c = 3.0$  m/s). [(a) and (b) combined.]
- (d) Angle between package velocity vector at package release and aircraft horizontal velocity vector,  $\epsilon_\phi$  ( $c = 5^\circ$ ).
- (e) Package velocity at package release,  $\epsilon_v$  ( $c = 5.0$  m/s).
- (f) Angle between package velocity vector at package release and aircraft horizontal velocity vector,  $\epsilon_\phi$  ( $c = 5^\circ$ ); package velocity at package release,  $\epsilon_v$  ( $c = 5.0$  m/s). [(d) and (e) combined.]
- (g) Ballistic model bias,  $B$  ( $B = -100$  m).
- (h) All parameter values, including  $B$ , divided by two.
- (i) All parameter values, including  $B$ , multiplied by two.



Table 7. Miss distance distribution for uniform components and selected departures from the nominal case.

	Miss distance (m) for nominal case and departures from it									
	Nominal	(a)	(b)	(c)	(d)	(e)	(f)	(g)	(h)	(i)
Average	461	312	417	254	441	453	434	480	235	892
90th percentile	699	571	636	437	667	685	653	747	358	1360
95th percentile	764	652	679	500	714	745	700	842	393	1490
99th percentile	885	788	762	596	817	851	793	1010	452	1800

Key to departures from nominal case:

- (a) Wind direction,  $\omega$  ( $c = 10^\circ$ ).
- (b) Wind velocity,  $\epsilon_w$  ( $c = 3.0$  m/s).
- (c) Wind direction,  $\omega$  ( $c = 10^\circ$ ); wind velocity,  $\epsilon_w$  ( $c = 3.0$  m/s). [(a) and (b) combined.]
- (d) Angle between package velocity vector at package release and aircraft horizontal velocity vector,  $\epsilon_\phi$  ( $c = 5^\circ$ ).
- (e) Package velocity at package release,  $\epsilon_v$  ( $c = 5.0$  m/s).
- (f) Angle between package velocity vector at package release and aircraft horizontal velocity vector,  $\epsilon_\phi$  ( $c = 5^\circ$ ); package velocity at package release,  $\epsilon_v$  ( $c = 5.0$  m/s). [(d) and (e) combined.]
- (g) Ballistic model bias,  $B$  ( $B = -100$  m).
- (h) All parameter values, including  $B$ , divided by two.
- (i) All parameter values, including  $B$ , multiplied by two.

#### 4. CONCLUSIONS

For the example drop test methodology and selected parameter values and errors, the probability that the package will impact within 881 m of a designated target is 99%. This distance is reduced to about 700 m for a 90% probability. Thus, tracking radar or cameras and impact recording cameras should be placed at correspondingly appropriate distances from the target, depending on the field-of-view capabilities of the cameras.

A sensitivity study indicates that the test parameter errors having the greatest effect on the probable miss distance are errors in velocity and direction of the wind and errors in initial velocity and direction of the test package. Thus, reducing these errors would have the most influence on reducing the probable miss distance.

Performing practice drops with dummy packages could improve the overall accuracy of the drop test and confidence in it. If test conditions and results of the practice drops were measured and used to improve data generated by the ballistics code (Ref. 2), a correction of the pallet/package assembly drop point could be determined.

The calculation method and equations given in this report are valid for other package drop methods, provided the number of parameter errors does not increase. If the number of parameter errors does increase, appropriate equations should be added. On the other hand, if fewer parameter errors exist, the appropriate error values can be set to zero.

Before conducting a drop test, probable miss distance values should be recalculated using parameter values and corresponding errors that are appropriate for the selected drop method. For some parameters, calibration tests may be necessary to obtain these values.

#### 5. REFERENCES

1. C. E. Walter, J. H. VanSant, and C. K. Chou, *Draft Criteria for Package Drop and Aircraft Crash Tests*, Lawrence Livermore National Laboratory, Livermore, CA, UCID-21697 (1989).
2. J. H. VanSant, *Ballistic Analyses of Free-Falling PAT Test Packages*, in preparation, Lawrence Livermore National Laboratory, Livermore, CA, PATC-IR 89-09 (1990).
3. S. F. Hoerner, *Fluid Dynamic Drag*, published by the author (1965).
4. "Drag Coefficients", *Mark's Standard Handbook for Mechanical Engineers*, 8th ed., pp. 11-68 and 11-69 (McGraw-Hill Book Co., New York, NY).

5. "Standard Atmosphere", *Mark's Standard Handbook for Mechanical Engineers*, 8th ed., pp. 11-58 and 11-59 (McGraw-Hill Book Co., New York, NY).
6. *Missile Engineering Handbook*, D. Van Nostrand Co., New York, NY, (1958), p. 56.